Towards mmWave Multistatic Arrays: A 120 GHz Phased-Array Imaging Radar

Ignacio Sardinero-Meirás[(1)], Ignacio E. López-Delgado[(1)], Elías Antolinos[(1)], Francisco N. Pérez-Fernández[(1)], Marta Ferreras[(1)], Lorena Pérez-Eijo[(2)], Marcos Arias[(2)], Borja González-Valdés[(2)], Jesús Grajal[(1)]
[(1)]Information Processing and Telecommunications Center, Universidad Politécnica de Madrid, Madrid, Spain
[(2)]Atlantic Research Center, Universidade de Vigo, Vigo, Spain
i.sardinero@upm.es

***Abstract*—The potential of single-node mmWave radar systems can be expanded with more sophisticated configurations, such as multi-frequency, multistatic, or phased-array radars. This paper presents a 120 GHz radar node, designed with a focus on transitioning to multistatic or phased-array setups, emphasizing scalability for integration into phased-array configurations. This involves addressing critical factors often overlooked, such as synchronization and data handling. A 120 GHz phased-array radar has been developed based on the custom-made single-node radar sensor. The array comprises 15 synchronized radar nodes with a Multiple-Input Multiple-Output setup. After a calibration procedure with a point-like target, the array is used to generate a range-crossrange image.**

***Index Terms*—Millimiter wave, LFMCW radar, phased array, multistatic radar.**

I. Introduction

Millimeter wave (mmWave) radar systems feature high-range resolution, high-gain small-sized antennas, non-ionizing radiation, day-and-night detection, penetration through obstacles, privacy preservation, and availability of commercial off-the-shelf components [1]–[3].

Among the short-range mmWave radars existing in the literature, single-node (monostatic) systems, with one transmitter and one receiver (Fig. 1a), have found application in various scenarios, including concealed weapon detection [4], [5], gait monitoring [6], vital sign monitoring [7], [8], and structural health monitoring [9]. Single-node radars are often integrated into multi-node radar networks to provide diverse perspectives when monitoring a specific scenario [10], [11].

However, traditional monostatic systems present some limitations [12]. For instance, slow mechanical systems are required for a high pixel resolution. Moreover, they misrepresent areas of the target where the specular reflection is oriented away from the incident direction. Finally, they cannot simultaneously monitor multiple targets in different locations. Consequently, the evolution of mmWave radar systems is pushing towards the development of multi-frequency, multistatic, and phased-array configurations:

- Multi-frequency radars, shown in Fig. 1b, harness the frequency-dependent properties of material penetration and range resolution [12]. They are not usually implemented because they involve the fabrication of one node at each frequency.

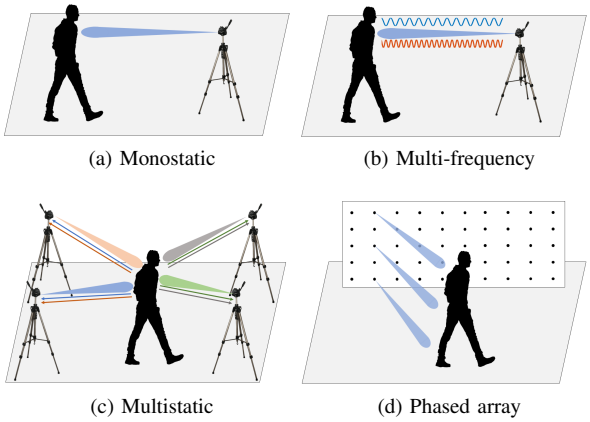

(a) Monostatic (b) Multi-frequency (c) Multistatic (d) Phased array

Fig. 1. Representation of different radar configurations.

- Multistatic radars, shown in Fig. 1c, display transmitters and receivers in different locations. They illuminate diverse target areas from different incidence angles, providing spatial diversity [13]. The primary challenge in multistatic radar systems lies in achieving a precise synchronization between the different nodes.
- Phased-array radars, shown in Fig. 1d, employ multiple transmitters and receivers to steer the radar beam. Digital phased arrays digitize the received signal at each transceiver antenna element. They enable the simultaneous and quick detection and tracking of several targets. Phased-array radars face the challenge of efficiently handling the vast amount of data generated [14].

This paper covers the key aspects in the design of mmWave radar nodes and their integration in multistatic and phased-array configurations, presenting a in-house developed multistatic phased array based on a custom-made single-node radar sensor [9].

II. Radar Nodes Design Considerations for Multistatic and Phased-Array Systems

Transitioning from monostatic mmWave radars to more sophisticated configurations, such as multi-frequency, multistatic, or phased-array radars, entails careful consideration of aspects such as synchronization, data handling, and calibration. In this section, important implications associated with each of these aspects are summarized.

1) Synchronization: Multistatic and phased-array radars demand precise synchronization among elements. This entails distributing a clock or local oscillator reference, and triggering all repetition intervals using a synchronized trigger signal. Commercial radars do not provide the possibility to introduce or extract reference or trigger signals. This complicates their synchronization.
2) Data handling: Multistatic and digital phased-array radars involve the management of significant data volumes. In multistatic radars, the vast amount of data extracted and processed is usually the bottleneck of the system. Poor data handling leads to either information loss or short captures. Commercial radar systems usually use processors, FPGAs or microcontroller units (MCUs) unable to process extensive data volumes.
3) Calibration: Fine calibration is critical for achieving accurate measurements with phased-array radars. There are several calibration techniques [14], often requiring a known target and an electromagnetically isolated environment to attain optimal results.

III. In-house developed 120 GHz radar node

This section presents a in-house developed LFMCW radar node operating at 120 GHz, which will be used as an element of a multistatic phased array. This node is designed keeping in mind the considerations outlined in the previous section. Thus, the main design requirements are:

- Trigger input to ensure synchronization between radar pulses.
- Clock reference inputs to ensure phase coherence.
- Analog in-phase and quadrature (IQ) outputs to be digitized with a commercial ADC.

The radar node consists of two main stages, handled in different printed circuit boards (PCB): the radiofrequency (RF) stage, and the intermediate-frequency (IF) stage.

The 120 GHz radar node [15] is shown in Fig. 2. The mmWave electronic components and antennas are integrated inside an MMIC from Indie Semiconductor [16]. The half power beamwidth of the integrated antenna is 60º. An external lens can be added to the radar to increase directivity.

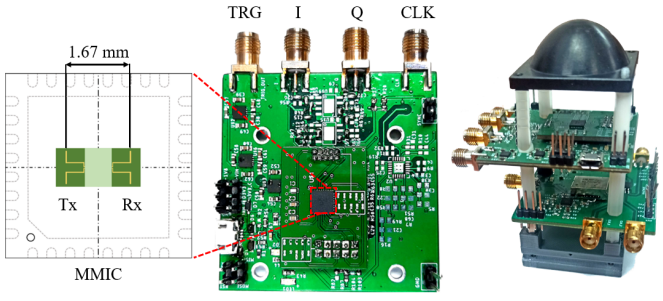

Fig. 2. In-house developed 120 GHz radar node proposed for a multistatic phased-array configuration. Printed-dipole antennas are integrated inside the MMIC [16]. Radar parameters such as bandwidth and sweep time are configurable: 0-20 GHz and 0.1-10 ms, respectively.

IV. In-house developed Multistatic Phased Array

A sparse multistatic linear phased-array radar has been developed based on the 120 GHz radar node. The array size aperture is fixed to 96 cm. Since a traditional densely-sampled array would result impractical in terms of hardware complexity and data handling [17], a sparse configuration with 15 nodes is selected. Eight nodes are used as transmitters and seven nodes are used as receivers[1]. Due to physical constraints, the minimum distance between elements is set to 2 cm = 8λ, where λ is the wavelength. The node positions are obtained by minimizing the side lobe level (SLL) of the array [18], and they are shown in Table I.

TABLE I
120 GHz array element positions along x-axis in centimeters.

Transmitters	±3.6	±10.8	±18.0	±25.2
Receivers	0	±16.0	±32.0	±48.0

The imaging performance of the designed array can be characterized with the point spread function (PSF), which is the response of the system to an ideal point-like target [18]. The PSF of the system at a certain point p_i can be obtained from the PSF of the transmitting and receiving arrays as shown in equations 1-3 [18], where κ_l is the wavenumber at the l-th frequency, t_m are the positions of the transmitters and r_n are the positions of the receivers.

$$PSF_{tx}(p_i) = \sum_{l,m} e^{-j\kappa_l |t_m - p_i|} \tag{1}$$

$$PSF_{rx}(p_i) = \sum_{l,n} e^{-j\kappa_l |r_n - p_i|} \tag{2}$$

$$PSF(p_i) = PSF_{tx}(p_i) \times PSF_{rx}(p_i) \tag{3}$$

For the positions given in Table I and a target placed at 3 meters, the simulated PSF is shown in Fig. 3. The diameter of the main lobe is approximately 1 cm and the SLL is 15 dB.

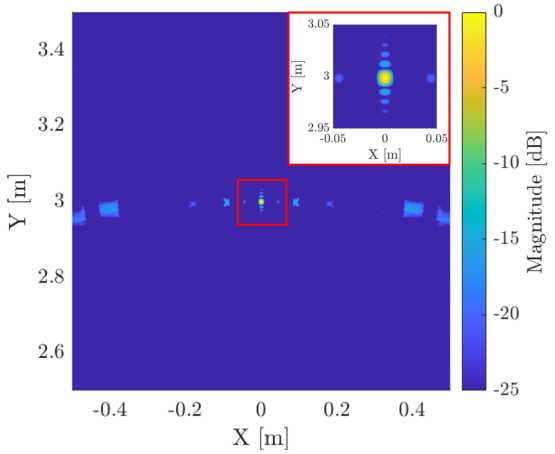

Fig. 3. Simulated PSF of the developed 120 GHz array for a target placed at 3 meters. The main lobe has a diameter of 1 cm and the SLL is 15 dB.

[1]This configuration, with multiple transmitters and multiple receivers, is commonly referred to as a Multiple-Input Multiple-Output (MIMO) radar.

The hardware architecture of the designed phased array is shown in Fig. 4. A reference clock signal is in-phased distributed to the 15 nodes. A copy of such clock signal is driven to an MCU and an external ADC via a programmable divider, which allows to configure the clock frequency of both devices independently. A demultiplexer module controlled by the MCU allows a correct distribution of the trigger signals. The MCU also drives a trigger signal to synchronize the system with the external ADC.

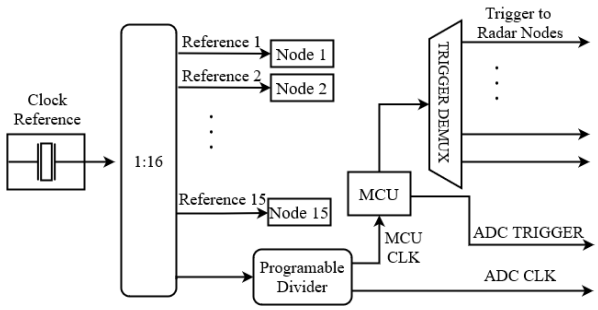

Fig. 4. Architecture of the designed 15-element phased array. A reference clock is driven to the radar nodes, the MCU and the external ADC. The MCU controls the radar nodes via a demultiplexer module and drives a trigger signal to the external ADC for capturing the data.

Fig. 5 shows the in-house developed multistatic phased array based on the 120 GHz radar node mounted on a tripod. As shown, 15 radar nodes are allocated in three separate PCBs. The central PCB accommodates the control unit alongside nine radar nodes, while the remaining six nodes are positioned on the side PCBs.

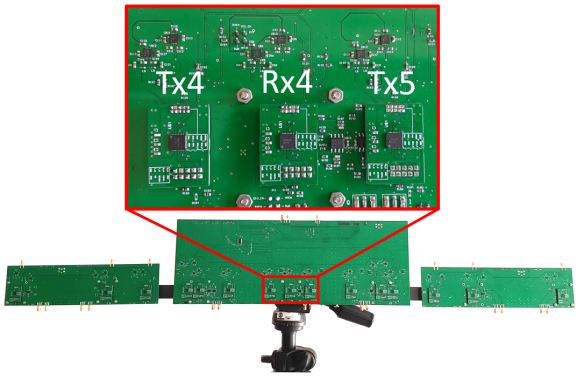

Fig. 5. 15-element multistatic phased array based on the 120 GHz radar node.

Due to different length of triggering signal paths, additional delays have been detected in each transmitter - receiver pair. This results in a wrong estimation of the target location. Therefore, such delays must be characterized to calibrate the system. For this purpose, a calibration measurement is performed. A metal cylinder is used as point like target. A cylinder scatters radiation uniformly in all directions, which implies that all echoes must have similar amplitudes. The calibration setup is shown in Fig. 6, where the cylinder is located 1 meter away from the array and aligned with the central receiver ($X = 0\ m$).

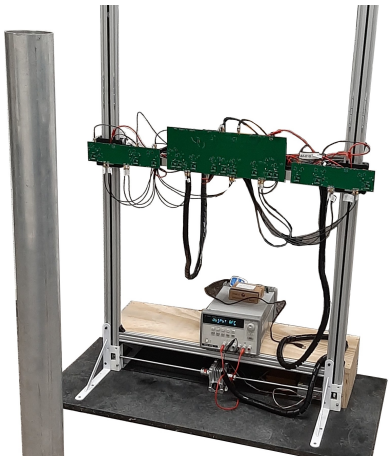

Fig. 6. Calibration setup. A metal cylinder is placed at 1 meter from the array and aligned with the central receiver.

The calibration results are shown in Fig. 7 for receiver Rx1. Prior to calibration (a), each transmitter generates a target echo at an inaccurate distance. Since with this setup all bistatic distances are known, a correction can be applied in each transmitter-receiver pair to obtain the correct distance. After calibration, accurate distance estimation is achieved across all transmitter-receiver pairs (b). This process is also extended to receivers Rx2-Rx7, but it is not shown here for simplicity.

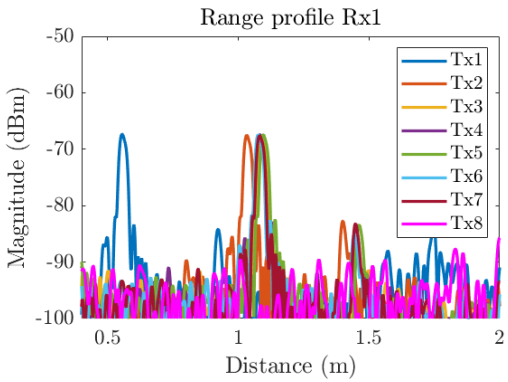

(a) Before calibration

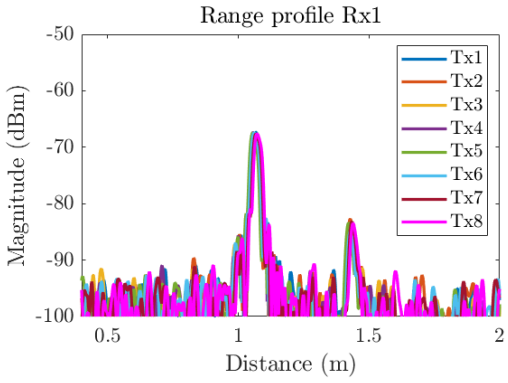

(b) After calibration

Fig. 7. Range profile obtained in receiver Rx1 for all transmitters with a metal cylinder located 1 meter away from the array.

After the calibration procedure, the developed array generates a range-crossrange image of a 30cm x 30cm metal plate. The plate is placed 1.5 meters away from the array, as shown in Fig. 8. Fig. 9 shows the resulting range-crossrange image from the measurement and the comparison with a simulation of the same scenario. As observed, results from the measurements are similar to the ones obtained in the simulation.

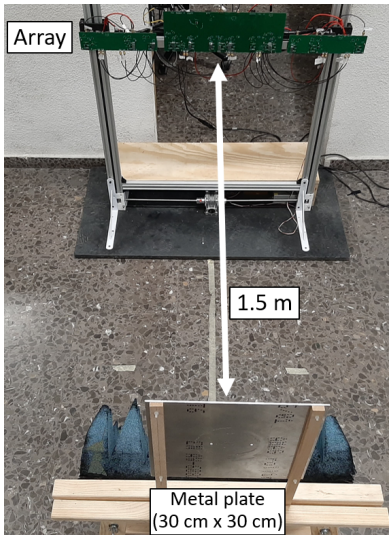

Fig. 8. Measurement setup. A 30cm x 30cm metal plate is placed 1.5 meters away from the array.

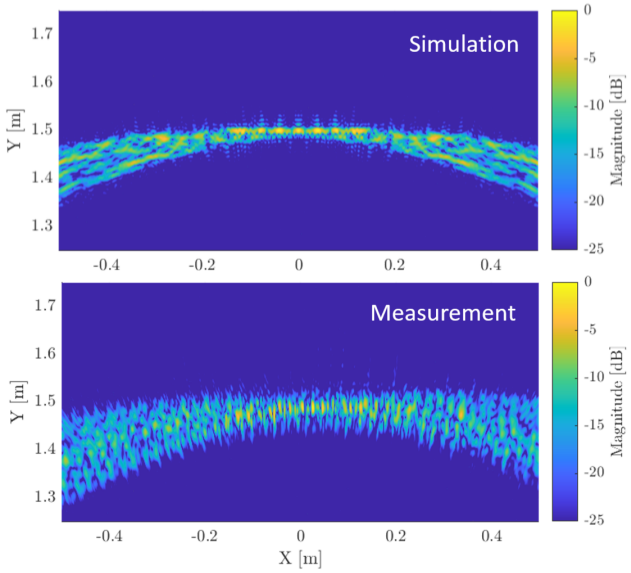

Fig. 9. Range-crossrange image of a 30cm x 30cm metal plate at 1.5 meters generated by the developed array. On the top: results from the simulation. On the bottom: results from the measurement.

V. Conclusion

Transitioning to multistatic and phased-array radars requires the consideration of the data processing and synchronization chains. A 120 GHz phased-array radar has been designed and manufactured based on a scalable 120 GHz radar node with trigger and reference oscillator inputs. Data volume has been considerably reduced by using a sparse-array configuration. The system has been successfully calibrated with a metal cylinder and has been used to generate a range-crossrange image of a metal plate.

Acknowledgment

This work was supported by the Spanish Ministry of Science and Innovation under projects PID2020-113979RB-C21 and PID2020-113979RB-C22 (MCIN/AEI/10.13039/501100011033). The work of I. Sardinero-Meirás was suported by a pre-doctoral Contract PRE2021-099967 from the Ministry of Science and Innovation. The work of Ignacio E. López-Delgado was supported by an FPU Fellowship granted by the Spanish Ministry of Education (FPU20/06405).

References

[1] M. G. Amin, Radar for indoor monitoring: detection, classification, and assessment, *1st ed. CRC Press*, 2018

[2] K.B. Cooper, and G. Chattopadhyay, "Submillimeter-Wave Radar: Solid-State System Design and Applications," *IEEE Microw. Mag.*, vol. 15, no. 7, pp. 51-67, 2014.

[3] C. Chaccour et al., "Seven Defining Features of Terahertz (THz) Wireless Systems: A Fellowship of Communication and Sensing," *IEEE Commun. Surveys Tuts.*, vol. 24, no. 2, pp. 967-993, 2022.

[4] K.B. Cooper et al., "A High-Resolution Imaging Radar at 580 GHz," *IEEE Microw. Wireless Compon. Lett.*, vol. 18, no. 1, pp. 64-66, 2008.

[5] J. Grajal et al., "3-D High-Resolution Imaging Radar at 300 GHz With Enhanced FoV," *IEEE Trans. Microw. Theory Techn*, vol. 63, no. 3, pp. 1097-1107, 2015.

[6] Z. Li et al., "Human Activity Classification with Adaptive Thresholding using Radar Micro-Doppler," in *2021 CIE Int. Conf. Radar*, Haikou, Hainan, China, 2021, pp. 1511-1515.

[7] G. Paterniani et al., "Radar-Based Monitoring of Vital Signs: A Tutorial Overview," *Proc. IEEE*, vol. 111, no. 3, pp. 277-317, 2023.

[8] E. Antolinos et al., "Cardiopulmonary Activity Monitoring Using Millimeter Wave Radars," *Remote Sens.*, vol. 12, no. 14, p. 2265, 2020.

[9] I. Sardinero-Meiras et al., "Portable Low-Cost Millimeter-Wave Radar Node for Short-Range Applications," in *2023 Eur. Radar Conf. (EuRAD)*, Berlin, Germany, 2023, pp. 1-4.

[10] I.E. López-Delgado et al., "mm-Wave wireless radar network for early detection of Parkinson's Disease by gait analysis," in *2023 IEEE Radar Conf. (RadarConf23)*, San Antonio, TX, USA, 2023, pp. 1-6.

[11] E. Antolinos, and J. Grajal, "Comprehensive Comparison of Continuous-Wave and Linear-Frequency-Modulated Continuous-Wave Radars for Short-Range Vital Sign Monitoring," *IEEE Trans. Biomed. Circuits Syst.*, vol. 17, no. 2, pp. 229-245, 2023.

[12] K. B. Cooper et al., "Penetrating 3-D Imaging at 4- and 25-m Range Using a Submillimeter-Wave Radar," *IEEE Trans. Microw. Theory Techn*, vol. 56, no. 12, pp. 2771-2778, 2008

[13] F. García-Rial et al., "Evaluation of Standoff Multistatic 3-D Radar Imaging at 300 GHz," *IEEE Trans. THz Sci. Technol.*, vol. 10, no. 1, pp. 58-67, 2020.

[14] C. Fulton, M. Yeary, D. Thompson, J. Lake, and A. Mitchell, "Digital Phased Arrays: Challenges and Opportunities," *Proc. IEEE*, vol. 104, no. 3, pp. 487-503, 2016.

[15] F. García-Rial, "Technological contributions to imaging radars in the millimeter-wave band," Ph. D dissertation, Dept. de Señales, Sistemas y Radiocomunicaciones, Univ. Politécnica de Madrid, Spain, 2019.

[16] Indie Semiconductor, "120 GHz Wide Band Transceiver – TRA_120_045," available at https://siliconradar.com/products/single-product/120-ghz-wide-band-transceiver-tra_120_045/

[17] B. Gonzalez-Valdes, Y. Rodriguez-Vaqueiro, Y. Alvarez, F. Las Heras, and A. Pino Garcia, "Nearfield-based array design for a realistic on-the-move personnel inspection system," in *2017 Eur. Radar Conf. (EuRAD)*, Paris, France, 2017, pp. 2846-2850.

[18] L. Perez-Eijo, M. Arias, B. Gonzalez-Valdes, Y. Rodriguez-Vaqueiro, O. Rubiños, A. Pino, I. Sardinero-Meirás, and J. Grajal, "Designing Advanced Multistatic Imaging Systems with Optimal 2D Sparse Arrays." *Applied Sciences*. **13** (2023),